Scattering of 22.3 MeV polarized protons from the even-mass cadmium isotopes $^{106\text{-}116}$Cd

J. Phys. G: Nucl. Part. Phys. 20 (1994) 1955–1972. Printed in the UK

Scattering of 22.3 MeV polarized protons from the even-mass cadmium isotopes $^{106-116}$Cd

R M A L Petit†, B W van der Pluym‡, P J van Hall§, S S Klein‖, W H L Moonen¶, G J Nijgh+, C W A M van Overveld* and O J Poppema‡

Experimental Nuclear Physics Group, Cyclotron Laboratory, Eindhoven University of Technology, Eindhoven, The Netherlands

Received 21 February 1994, in final form 11 July 1994

Abstract. Measurements have been done on polarized-proton scattering from the even-mass cadmium isotopes $^{106-116}$Cd, at a beam energy of 22.3 MeV. The experimental data were analysed using first- and second-order vibrational models in a coupled-channels formalism. The 0_1^+, 2_1^+ and 3_1^- levels are represented satisfactorily by theory. In $^{106-114}$Cd the 2_2^+ and 4_1^+ levels were resolved; for the 2_2^+ levels the theory systematically underestimates the first diffraction maximum of the cross section at 30° while the 4_1^+ levels are reproduced reasonably well. In $^{112-114}$Cd the 0_2^+ level could also be studied; there are indications for a strong coupling between the two-phonon 0^+ state in the ground-state band and the 0^+ head of the intruder band. In ^{114}Cd we also investigated the 2_3^+ level, probably the first excited state of the intruder system, which showed an angular pattern with more pronounced details than the 2_1^+ states. Finally in ^{112}Cd the 1_1^- and 5_1^- levels were studied which have a strong direct coupling to the ground state.

NUCLEAR REACTIONS ^{106,108,110,112,114,116}Cd (polarized p,p') E = 22.3 MeV; measured $\sigma(\theta)$, $A(\theta)$; deduced optical model parameters, deformation strengths. CC calculations in vibrational model.

1. Introduction

The even cadmium isotopes exhibit intriguing properties. At first sight they seem to be examples of vibrational nuclei, being two protons away from the closed $Z = 50$ shell. High-resolution gamma spectroscopy [1–3], however, has revealed in some nuclei the existence of a quintet of states at the position of the two-phonon triplet showing the additional levels 0^+ and 2^+. It seems obvious that these levels are intruder states originating from a 2p–2h

† Present address: Philips Industrial Electronics BV, Unit EMT, Eindhoven, The Netherlands.

‡ *Present address: R. de Graafweg 500, 2625 DP Delft, The Netherlands.*

§ Now at Semiconductor Physics Group, Faculty of Physics, Eindhoven University of Technology, Eindhoven, The Netherlands.

‖ Now at Nuclear Physics Techniques Group, Cyclotron Laboratory, Eindhoven University of Technology, Eindhoven, The Netherlands.

¶ Present address: Hoogovens Groep BV, IJmuiden, The Netherlands.

+ Retired.

* Now at Faculty of Mathematics and Computing Science, Eindhoven University of Technology, Eindhoven, The Netherlands.

‡ Deceased.

0954-3899/94/121955+18$19.50

excitation over the nearly closed $Z = 50$ shell. For example, the 0_2^+ states that we studied in ^{112,114}Cd are nowadays regarded as the basis of an intruder band rather than as a member of the 'regular' two-phonon triplet. The amount of mixing between the two configurations then becomes an important question.

Clearly, complicated nuclear models have to be invoked in such a situation. One of the few possibilities is the IBA-2 model with configuration mixing as developed by Duval and Barrett [4] and applied to the cadmium isotopes by Heyde *et al* [5]. These authors obtain as a result that the 0_2^+ and 0_3^+ states in ^{112,114}Cd contain both configurations with equal strength. O'Donnell *et al* [6] have analysed their (t,p) data for ^{110,112,114}Cd in terms of interacting vibrational and rotational configurations. The three lowest 0^+ states were found to be relatively pure. Casten *et al* [7] have pointed to an important ambiguity: it is possible that the normal and intruder states are strongly mixed but that due to cancellation of amplitudes the γ-ray transitions nevertheless suggest rather pure configurations. A similar cancellation may also occur in the (t,p) amplitudes.

The close spacing of the levels of the quintet, however, hampers the study by means of nuclear reactions, as compared with high-resolution γ-ray spectroscopy. Moreover, in the analysis of hadron experiments the assumptions that have to be made regarding the reaction mechanism introduce additional uncertainties in coupling scheme and transition densities. On the other hand, interference between different reaction paths may possibly enhance the sensitivity of a scattering experiment and so help in the analysis and interpretation.

We have used the polarized-beam facility of the Eindhoven University of Technology (EUT) cyclotron to perform $(\vec{p}, p')$ reactions on the even-mass cadmium isotopes $^{106-116}$Cd. In the next section an outline of the experimental set-up is given. We then proceed with the analysis of the experimental data using coupled-channels calculations. We discuss our results and simultaneously compare them with conclusions derived from other experiments. The final section contains a short summary.

Earlier measurements on the 0_1^+, 2_1^+ and 3_1^- states of ^{110,112,114}Cd at 20.4 MeV beam energy have been published by Wassenaar *et al* [8]. Partial results of the present study have been communicated at the Osaka conference [9]. For a further listing of the literature on the cadmium isotopes discussed in this paper we refer the reader to the compilations in Nuclear Data Sheets [10–15].

2. Experimental procedure

The experiments were done using the polarized-proton facility of the Eindhoven cyclotron. Details of the apparatus have been given by Moonen *et al* [16] and in earlier publications cited there. Most of the present experiments were carried out with a proton beam of 22.3 MeV energy, 20 keV energy spread (FWHM), about 20 nA intensity at the target and about 20 mm mrad beam quality.

The scattered protons were detected by 3 mm thick lithium-drifted silicon detectors [17] that were cooled by a Peltier device. The energy width (FWHM) of the lines in the observed proton spectra amounted to 38 keV when transmitted through the target foil and to 47 keV when reflected.

The beam polarization was reversed every few minutes during an experimental run. The degree of polarization was continuously monitored; usually it was about 90%. Measuring periods of about 15 hours were needed for every angle setting in order to obtain at least 500 counts of protons leaving the target nuclei in each of the assumed two-phonon states.

Targets were self-supporting metallic foils, of thickness 600–1000 μg cm^{-2} and isotopic purity 96–98%, except for the rare isotopes ^{106}Cd and ^{108}Cd which were 91 and 64% pure,

respectively.

In the spin-up and spin-down spectra obtained, the peak intensities were integrated by adding the contents of the channels between two peak markers chosen by visual inspection. Multiplets of nearby lying and overlapping peaks were fitted by an analytical curve consisting of the superposition of a Gaussian and a Lorentzian form. A minimal error of 2% was assumed in the values of cross section and analysing power, due to the normalization procedure.

From these experiments data could be extracted for the ground states and the one-phonon states 2_1^+ and 3_1^- for all isotopes studied, except for the 3_1^- state in ^{108}Cd. Also, we could obtain results for a number of two-phonon states 0_2^+, 2_2^+, 4_1^+ and even the 5_1^- and 1_1^- levels of ^{112}Cd. All analysed levels have been listed in table 1.

Table 1. Levels in the cadmium isotopes studied in this paper.

J^π	$A = 106$	108	110	112	114	116
1_1^-				2.507		
5_1^-				2.373		
3_1^-	2.371		2.079	2.005	1.958	1.922
2_3^+					1.364	
4_1^+	1.494[a]	1.508[a]	1.542	1.415	1.283	
2_2^+	1.717[a]	1.602[a]	1.476	1.312	1.210	
0_2^+				1.224	1.134	
2_1^+	0.633	0.633	0.658	0.617	0.558	0.513
0_1^+	0	0	0	0	0	0

All excitation energies given in MeV.

[a] Note inverted order.

When our experiments were done we were not aware of the additional levels mentioned in [1] and [2]. This might cause some difficulties in the interpretation of our results: specifically, the 2_2^+ level at 1.476 MeV in ^{110}Cd is not resolved from the 0_2^+ level, and the 4_1^+ level at 1.415 MeV in ^{112}Cd is very close to the 0_3^+ level at 1.433 MeV. The scattering patterns $d\sigma/d\Omega$ and $A(\theta)$ for 2_2^+, ^{110}Cd (figures 6 and 7), show a rather similar behaviour to that for the neighbouring isotopes where no close contaminating levels are present, so that we conclude that the 0_2^+ contribution to the 2_2^+ level in ^{110}Cd is weak. For 4_1^+, ^{112}Cd, the 0_3^+ admixture might be responsible for the increase of the cross section at the very forward angles. Also, the 3_1^- states in all isotopes have more or less closely adjacent states which, however, do not seem to disturb the angular distribution calculated for a 3^- level (see figure 5).

3. Results and discussion

3.1. The vibrational model: concepts and notation

Before presenting our results and their analysis we wish to review briefly a few of the concepts involved [18]. If the target nucleus is spherically symmetric but susceptible to vibrations, the radius vector $R(\theta, \phi)$ of the nuclear surface may be written as

$$R = R_0 + \delta R = R_0 \left(1 + \sum_{\lambda,\mu} \alpha_{\lambda\mu} Y_{\lambda\mu}(\theta, \phi) \right). \tag{1}$$

The parameters $\alpha_{\lambda\mu}$ can be expressed in phonon creation and annihilation operators:

$$\alpha_{\lambda\mu} = \frac{\beta_\lambda}{\sqrt{2\lambda+1}}[a_{\lambda\mu} + (-1)^\mu a^\dagger_{\lambda\mu}] \tag{2}$$

in which β_λ is a parameter for the amplitude of the vibration. If we insert expression (1) into the projectile–target interaction and perform a Taylor expansion we obtain

$$V = V_0 + \frac{\partial V_0}{\partial R}(\delta R) + \frac{\partial^2 V_0}{\partial R^2}\frac{(\delta R)^2}{2} + \ldots \tag{3}$$

in which V_0 is the standard optical potential. Insertion of expression (3) into the Schrödinger equation will result in a set of coupled-channels equations in which the non-spherical terms couple the various excited states of the target nucleus.

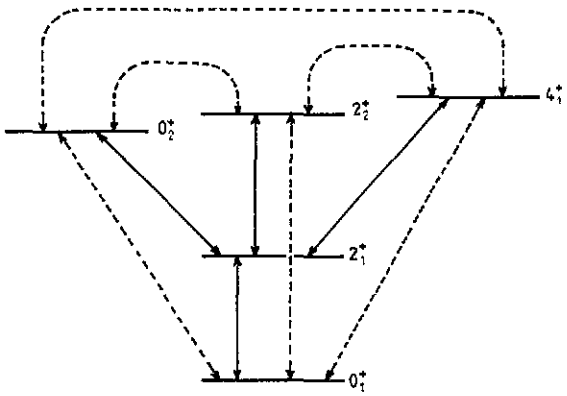

Figure 1. *Illustration of first-order and second-order vibrational coupling. Full arrows,* V1 transitions; broken arrows, additional transitions in V2.

Depending on whether we retain only the first-order term or also take into account the second-order terms we obtain a different coupling scheme. In our analysis we denote these possibilities by V1 and V2, respectively. From equations (2) and (3) it is clear that in V1 we only couple states that differ by one phonon, while in V2 we introduce additional transitions between states that differ by zero or two phonons. This is elucidated by figure 1, which shows the situation for $L = 2$ phonons.

So far, the two-phonon states have been considered as ideal. In practice, they may contain one-phonon components allowing for a direct first-order excitation from the ground state. For example, the 2^+ state may be represented [19] as

$$|2^+\rangle = \cos\phi|\text{one-phonon}\rangle + \sin\phi|\text{two-phonon}\rangle.$$

In our analyses we allowed for such mixing and we used ϕ as an adjustable parameter, $\phi = 90°$ corresponding to a pure two-phonon state. Also, we introduced additional strength parameters for the direct transition as defined by Tamura [18].

3.2. Elastic scattering, the strong 2^+ and 3^- states

First we analysed the elastic data together with the inelastic data for the 2^+_1 and 3^-_1 states using the extended optical model [20, 21]. In short: the parameters of the optical model were fitted to the elastic cross section and the analysing power, using the deformation parameters β_2 and β_3, estimated from the strength (i.e. the height of the first maximum of

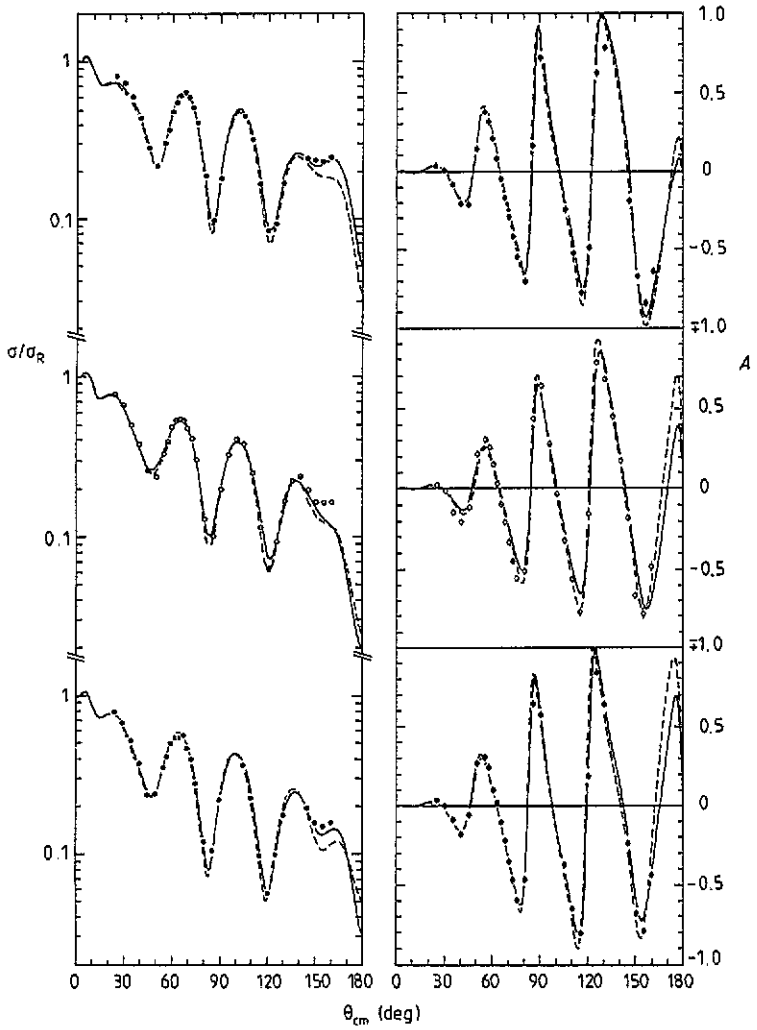

Figure 2. Elastic scattering from the even-mass cadmium isotopes ^{106,108,110}Cd (top to bottom). Full curves, first-order vibrational model; broken curves, second-order vibrational model.

the cross section) of the 2_1^+ and 3_1^- states (if available). Afterwards, β_2 and β_3 were adjusted to the complete 2_1^+ and 3_1^- data. If necessary, this process was iterated. In the coupled-channels analysis we tried both the first-order and the second-order vibrational models. The experimental data together with the theoretical curves are shown in figures 2–5 (these figures, however, have been computed at a later stage, where also couplings to the so-called two-phonon states (0_2^+), 2_2^+ and 4_1^+ were included). The corresponding parameters of the optical potential can be found in table 2 while the deformation parameters are listed in table 3.

The description of the elastic scattering (figures 2 and 3) is very satisfactory, as expected. The extracted parameters do not exhibit specific irregularities that would point to a change in the underlying nuclear structure with increasing neutron number. The step-like increase of the real potential, when going from ^{110}Cd to ^{112}Cd, is compensated by a small decrease of the real radius so that the volume integral behaves well. A similar remark holds for the

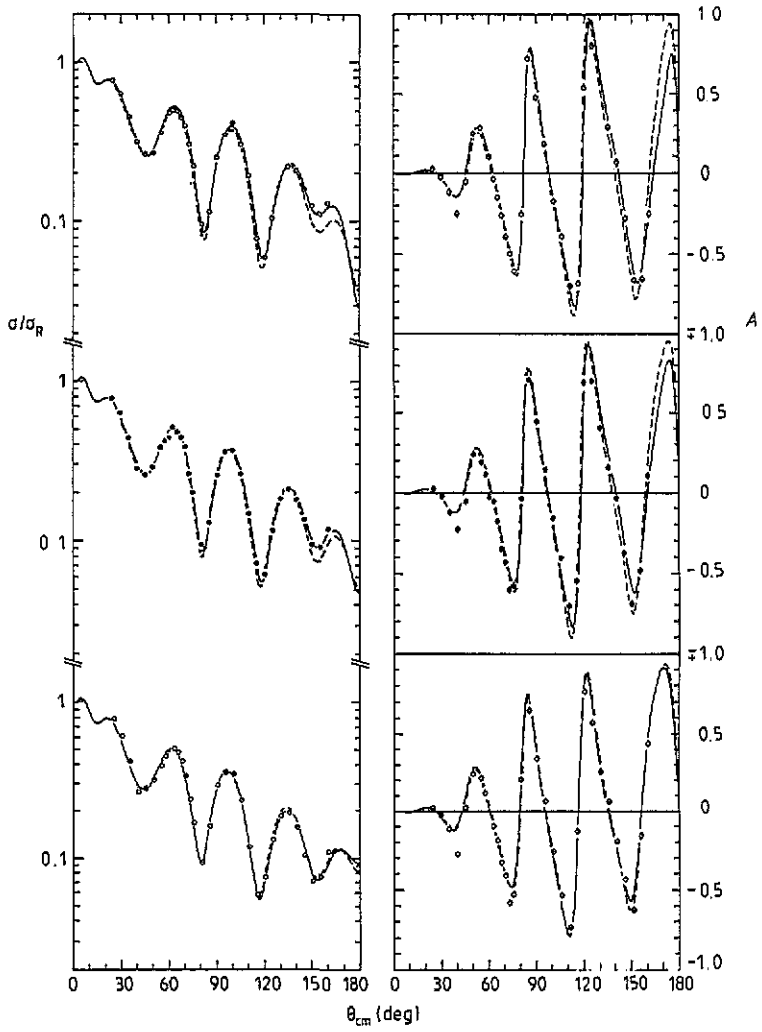

Figure 3. Elastic scattering from the even-mass cadmium isotopes ^{112,114,116}Cd (top to bottom). Full curves, first-order vibrational model; broken curves, second-order vibrational model.

spin–orbit potential.

The agreement between experiment and theory for the 2_1^+ states is satisfactory as well, especially since only the height of the first maximum of the cross section was included in the fitting procedure (figure 4). When we compare the first-order (V1) and the second-order (V2) vibrational calculations we see a slight preference for the V1 model in ^{106}Cd, whereas $^{108-116}$Cd are reproduced better by the V2 calculations. This difference is mainly based on the analysing powers at backward angles.

In previous work on $^{110-114}$Cd [8] we encountered difficulties in the description of the backward cross sections and analysing powers for the 3_1^- states. The data points in the present paper are of much better quality, but the general discrepancy remains (figure 5). The differential cross section and the analysing power for angles larger than 120° show a stronger oscillatory behaviour than the calculations, though the discrepancies are not as large as those with the DWBA calculations in [8]. The 3_1^- states depicted in figure 5 do not

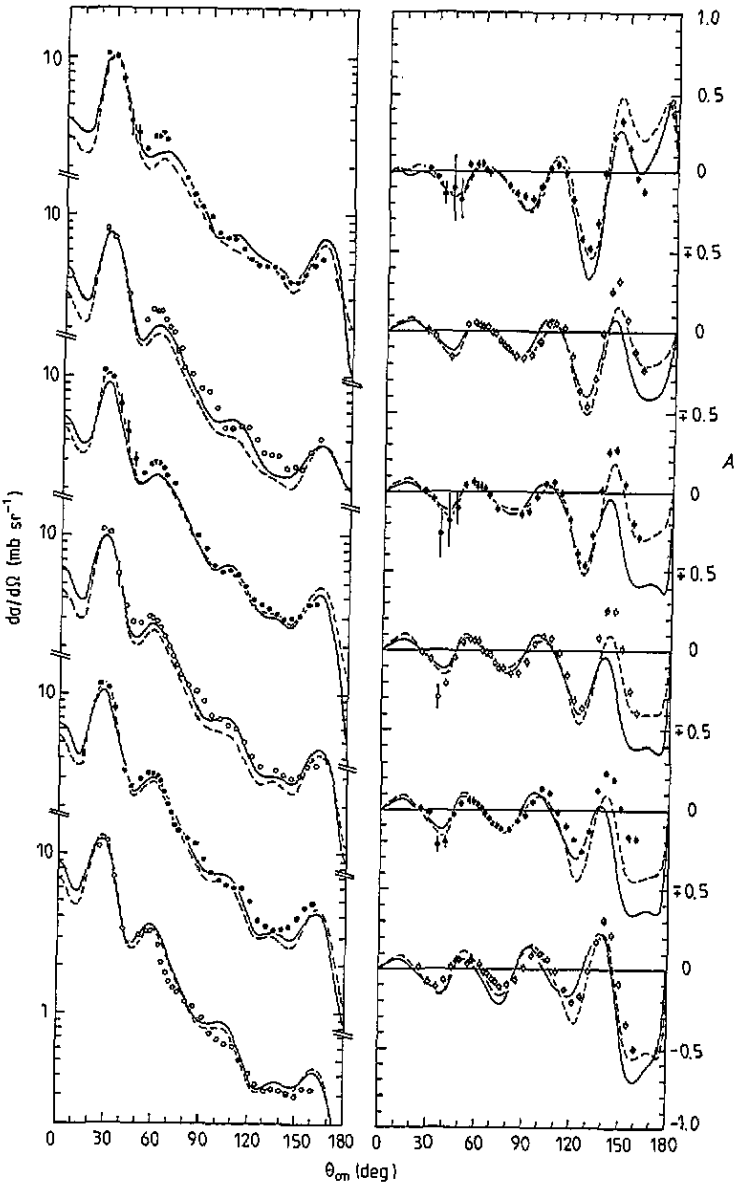

Figure 4. Inelastic scattering from the even-mass cadmium isotopes ^{106}Cd (top) to ^{116}Cd (bottom), exciting the 2_1^+ state. Full curves, first-order vibrational model; broken curves, second-order vibrational model. CC scheme: 0232_24.

show a clear preference for V1 or V2, in contrast to the situation for the 2_1^+ state.

Because of the difficulty in reproducing the general slope of the cross section in the 3_1^- data we have tried the inversion procedure for the form factor as developed by Van Overveld and Van Hall [22] for the isotopes ^{106}Cd and ^{110}Cd. The results have been published earlier by Van Overveld [23]. As expected, the cross section curves and to a lesser extent the analysing power curves are reproduced better than before, using a conventional form factor, but only in the imaginary coupling for ^{106}Cd does the form factor derived from the

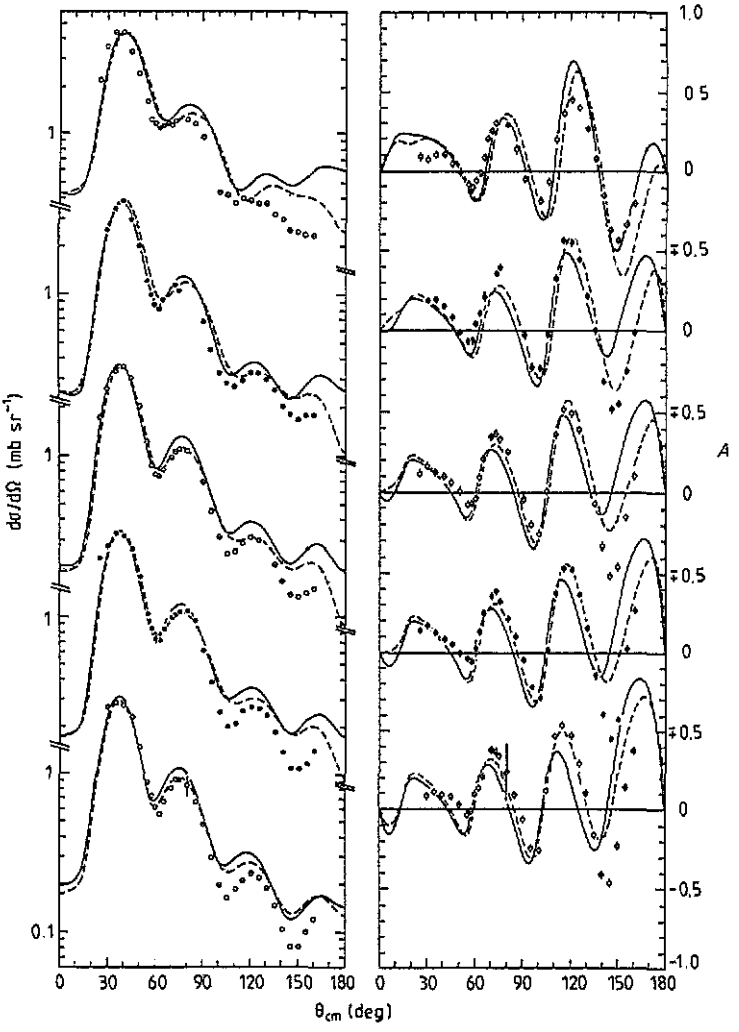

Figure 5. Inelastic scattering from the even-mass cadmium isotopes ^{106}Cd (top) and ^{110}Cd to ^{116}Cd (bottom), exciting the 3_1^- state. (No data available for ^{108}Cd). Full curves, first-order vibrational model; broken curves, second-order vibrational model. CC scheme: 0232_24.

inversion algorithm show a significant deviation from the conventional one.

Apart from our previous work [8] we can compare the present results with the systematic studies of Lutz *et al* [24] at 14 MeV, Makofske *et al* [25] at 16 MeV and Cereda *et al* [26] at 22.3 MeV. These experiments were done with unpolarized protons. There exist some other (p,p') experiments but these often concern only a single isotope, e.g. [27] and [28].

When comparing our experimental points for the cross section with those of Cereda *et al* [26] we observe a general agreement of the curve shapes. There are, however, a few conspicuous differences:

(i) In elastic scattering from isotope ^{116}Cd our maximum at 135° is higher than Cereda's and our minimum at 150° is shallower.

(ii) In the 2_1^+ curves we observe higher maxima at 60° and 150° in $A = 106$ and at 60° in $A = 110$; we do not observe Cereda's maximum at 80° in $A = 116$.

Table 2. Optical-model parameters from a coupled-channels analysis using the extended optical model.

A	Model[a]	V_r	r_r	a_r	W_D	r_i	a_i	V_{so}	r_{so}	a_{so}
106	V1	53.67	1.16	0.68	7.88	1.32	0.67	5.58	1.02	0.68
	V2	54.01	1.16	0.69	9.48	1.30	0.59	5.46	1.01	0.63
108	V1	54.36	1.18	0.67	10.09	1.24	0.68	5.68	1.10	0.54
	V2	54.69	1.17	0.67	10.65	1.26	0.63	5.64	1.11	0.45
110	V1	54.94	1.17	0.66	7.82	1.27	0.74	5.58	1.05	0.59
	V2	54.68	1.17	0.67	9.50	1.26	0.63	5.52	1.09	0.52
112	V1	56.56	1.15	0.69	8.19	1.27	0.75	6.06	1.06	0.60
	V2	56.95	1.14	0.70	9.65	1.26	0.67	6.06	1.09	0.51
114	V1	56.58	1.14	0.71	8.49	1.26	0.76	6.15	1.07	0.64
	V2	56.74	1.14	0.71	9.95	1.26	0.66	6.26	1.10	0.55
116	V1	55.52	1.17	0.68	8.73	1.24	0.76	5.87	1.02	0.70
	V2	56.30	1.15	0.69	10.09	1.25	0.67	6.12	1.06	0.66

All energy values in MeV; all lengths in fm.
Coulomb radius constant $r_C = 1.25$ fm; volume absorption $W_V = 0$.
[a] V1, V2 are the first- and second-order vibrational models, respectively.

Table 3. Quadrupole (β_2) and octupole (β_3) deformation strengths for the central and spin–orbit parts of the potential. The spin–orbit to central enhancement β_{so}/β_c is given by λ_2 and λ_3, respectively.

A	Model[a]	β_{2c}	β_{3c}	β_{2so}	β_{3so}	λ_2	λ_3
106	V1	0.16	0.17	0.21	−0.109	1.26	−0.64
	V2	0.16	0.17	0.13	−0.065	0.80	−0.37
108	V1	0.16	0.16[b]	0.26		1.64	
	V2	0.15	0.16[b]	0.27		1.78	
110	V1	0.16	0.15	0.24	0.004	1.46	0.03
	V2	0.16	0.16	0.16	0.030	0.94	0.19
112	V1	0.17	0.16	0.24	−0.060	1.39	−0.38
	V2	0.17	0.16	0.26	0.007	1.51	0.04
114	V1	0.18	0.15	0.30	−0.128	1.67	−0.84
	V2	0.18	0.16	0.31	−0.052	1.75	−0.33
116	V1	0.18	0.14	0.26	−0.061	1.44	−0.44
	V2	0.18	0.14	0.25	−0.058	1.37	−0.41

[a] V1, V2 are the first- and second-order vibrational models, respectively.
[b] These values could not be fitted for lack of experimental data; they were chosen so as to obtain a reasonable set of OM parameters.

(iii) In our 3_1^- curves the maxima at 70, 120 and 155° in ^{106}Cd are less pronounced than in Cereda's paper; also, we find a shallower minimum at 145° in ^{116}Cd.

While statistics in our experiment are usually better than 2% in the individual points, we notice some normalization differences (up to 35% but usually less than 20%) between our values and Cereda's. This normalization originates from the extrapolation to $\theta = 0$ of the σ/σ_R curves in the elastic scattering experiments (figures 2 and 3). In constructing these curves, Cereda (tables III, V and VI of [26]) and ourselves (table 2 of this paper) have arrived at slightly different sets of OM parameters. The most important discrepancy was the sharper surface of the real potential in our set, which was necessary in order to account for the amplitude of the oscillations in the analysing power data for the elastic scattering. Also, Cereda and ourselves have used different procedures assigning fixed values to constants

or having them produced by the fitting algorithm. Finally, we must keep in mind that an adjustment error of the scattering angle of 0.1 degree at 20° would bring about an error of 2% in the Rutherford cross section due to the factor $\sin^4(\theta/2)$.

Due to all these considerations, we find it hard to pinpoint the cause of the normalization differences.

The deformation parameters β_2 and β_3 found by us (table 3) are systematically lower than those reported by Lutz *et al* [24], possibly because of the lower beam energy used in that experiment. Differences of β_2 and β_3 as derived by us with the results of Makofske *et al* [25] and Cereda *et al* [26] remain within a reasonable limit of 10–15%. The same remark applies to the density moments that can be derived from the optical-model and deformation parameters. Our values are 10–20% lower than Cereda's, which might be due to the sharper nuclear surface as 'seen' in our experiment.

3.3. The two-phonon multiplets

Next we analysed the assumed two-phonon multiplets (0_2^+, 2_2^+, 4_1^+). In the calculations we allowed for a one-phonon component mixed into these states (see section 3.1). In table 4 we list the parameter values resulting from our analysis while in figures 6–10 the computed angular distributions are compared with the experimental data. It should be noted that the mixing parameters were determined by a fit to both cross section and analysing power over the whole angular region.

From figures 6 and 7 we can see that this procedure systematically underestimates the 2_2^+ cross section at the forward maximum around 30°. An increase of the one-phonon component might perhaps remove this discrepancy but only at the expense of the analysing power. Due to the dominance of the direct one-phonon transition in that case, the analysing power (and also the cross section) for the 2_2^+ state would tend to be more similar to that for the 2_1^+ level (figure 4), so that the strong oscillations observed in all experimental data of both cross section and analysing power for the 2_2^+ states would no longer be reproduced. Apart from this problem the agreement between experiment and theory can be considered as rather good.

When we look at the phase of the oscillatory pattern there seems to be a slight preference for the first-order vibrational model. The mixing angles in table 4 indicate a predominant two-phonon character of the 2_2^+ states. The small one-phonon component, however, may be responsible for most of the excitation strength observed in the experiment.

From the inspection of figures 6 and 7 our results for all of the 2_2^+ states appear to be very similar. Kumpulainen *et al* [1], however, find a ratio between the $B(E2)$ values to the 2_1^+ level and those to the ground state which increases with neutron number, pointing to a purer two-phonon character of the second 2^+ state in the heavier cadmium isotopes.

The data for the 4_1^+ states (figures 8 and 9) exhibit some scatter and sometimes have rather large uncertainties. The differential cross sections show little structure, with the exception of ^{114}Cd. The gross structure is reproduced by theory, but sometimes details are being missed, as in ^{114}Cd. Both cross section and analysing power point in the direction of the second-order model. From table 4 we note that, with the exception of ^{106}Cd and the V2 calculation for ^{114}Cd, the mixing angles scatter around ±90°, indicating a rather pure two-phonon state. In these exceptions we need a destructive interference in order to account for the small cross sections. A purely two-phonon calculation, however, also describes the data reasonably well. From this we conclude that all the 4_1^+ levels investigated can be considered as rather pure two-phonon states. The coupled-channels calculations give a fair description of the data. In contrast to the 2_2^+ states, a slightly improved fit was achieved

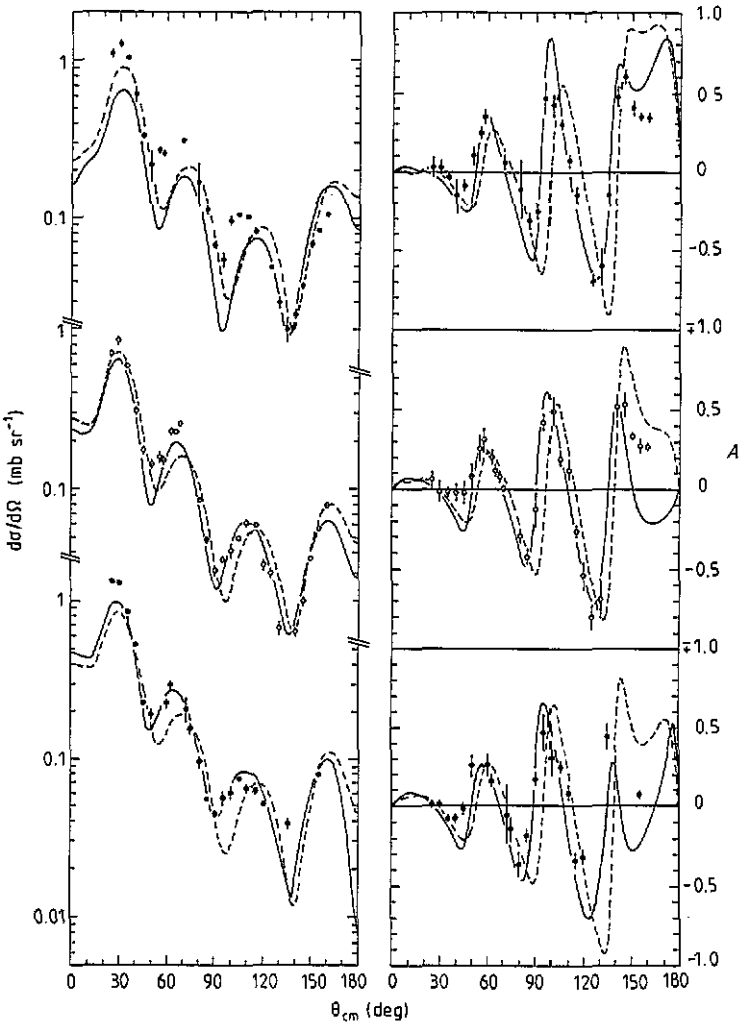

Figure 6. Inelastic scattering from ^{106,108,110}Cd (top to bottom), exciting the 2_2^+ state. Full curves, first-order vibrational model; broken curves, second-order vibrational model. cc scheme: 0232_24 including one-phonon component mix.

when using second-order vibrators.

In two cases (^{112}Cd and ^{114}Cd) we could obtain data for the 0_2^+ state (figure 10). These states are of particular interest since they are believed to be the ground state of the intruder configurations and not the 0^+ member of the 'regular' two-phonon multiplet [1]. The excitation mechanism of such states by inelastic scattering is unclear unless we allow for components in the wavefunction that originate from the 'normal' (i.e. ground-state band) configuration.

The mixing angles for the 0_2^+ states (table 4) have values around 135° and therefore indicate that a strong one-phonon component is needed in order to describe the data. A detailed inspection of the calculations showed nevertheless that the two-phonon component dominates cross section and analysing power. The direct transition is rather weak in itself. This leads to large errors in the mixing angle when we fit the experimental data by including

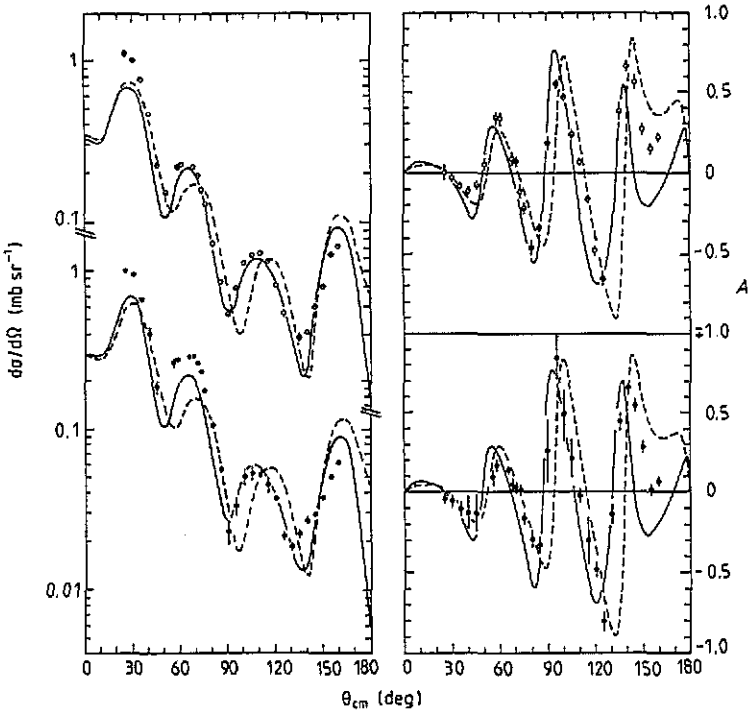

Figure 7. Inelastic scattering from ^{112}Cd (top) and ^{114}Cd (bottom), exciting the 2_2^+ state. Full curves, first-order vibrational model; broken curves, second-order vibrational model. CC scheme: $0230_2 2_2 4$ including one-phonon component mix.

this negatively interfering transition. On the other hand the presence in these levels of only 50% of the two-phonon strength points to a strong mixing between the 0^+ intruder state and the 0^+ two-phonon state.

These findings are in good agreement with the theoretical results of Heyde *et al* [5]. So we think that we indeed have here the peculiar situation pointed out by Casten *et al* [7] that we referred to in the introduction. It should be emphasized that this conclusion is based on the argument of overall excitation strength only.

In all these calculations we have used as transition densities the first and/or second derivatives of the optical potential. There is some evidence that the form factor may be located more inside the nucleus: Wesseling *et al* [29] find a smaller radius of the transition charge density in an (e,e′) experiment on ^{110}Cd for the 4_1^+ level as compared with higher 4^+ states, and Cereda *et al* [26] obtain a better fit for the 2_2^+ states in cadmium when decreasing the radius parameter for the second derivative. It is clear that, by relaxing the OM prescriptions for the transition densities, one introduces a number of additional parameters. Therefore we have not investigated these possibilities.

3.4. Some other states

We could also extract data for a few other states from the collected proton spectra. The first one is the 2_3^+ level at 1.364 MeV in ^{114}Cd (figure 11). This state is of particular interest since it is interpreted as the first excited state of the intruder band [1]. The experimental cross section shows a rather oscillatory pattern at forward angles. This pronounced structure

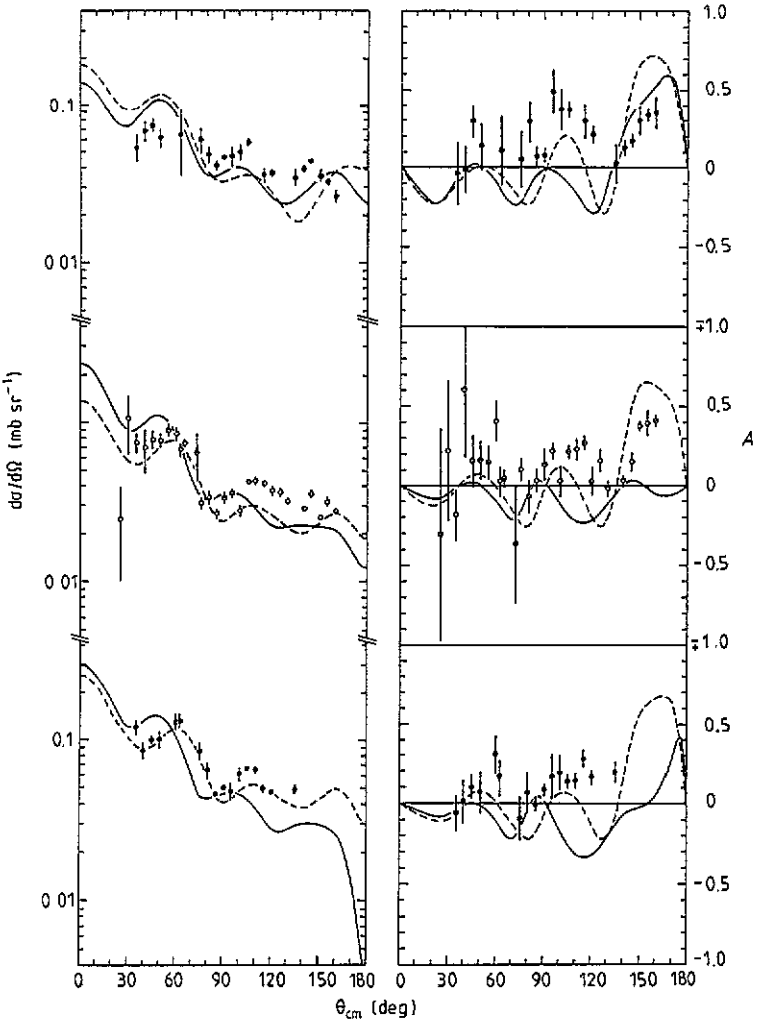

Figure 8. Inelastic scattering from ^{106,108,110}Cd (top to bottom), exciting the 4_1^+ state. Full curves, first-order vibrational model; broken curves, second-order vibrational model. CC scheme: 0232_24 including one-phonon component mix.

also shows up in the results of Lutz *et al* [24], obtained at 14 MeV beam energy. Such a sharp pattern can arise only either from two interfering reaction paths that have different transition densities or from two competing mechanisms in the same channel.

For the analysis we used the same procedure as for the 2_2^+ states, outlined above. Clearly the oscillatory structure cannot be described by the calculations. A purely one-phonon calculation does at least reproduce the cross section maxima more or less but the small cross section value indicates that the direct coupling to the ground state is very weak. On the other hand the analysing power is described better when also a two-phonon component is present.

Obviously the coupling scheme is too simple. Above, we concluded that there is strong mixing between the 0_2^+ and 0_3^+ states. Hence, two nearly equivalent paths for exciting the 2_3^+ state are possible, namely $0_1^+ \rightarrow 2_1^+ \rightarrow 0_2^+ \rightarrow 2_3^+$ and $0_1^+ \rightarrow 2_1^+ \rightarrow 0_3^+ \rightarrow 2_3^+$. One

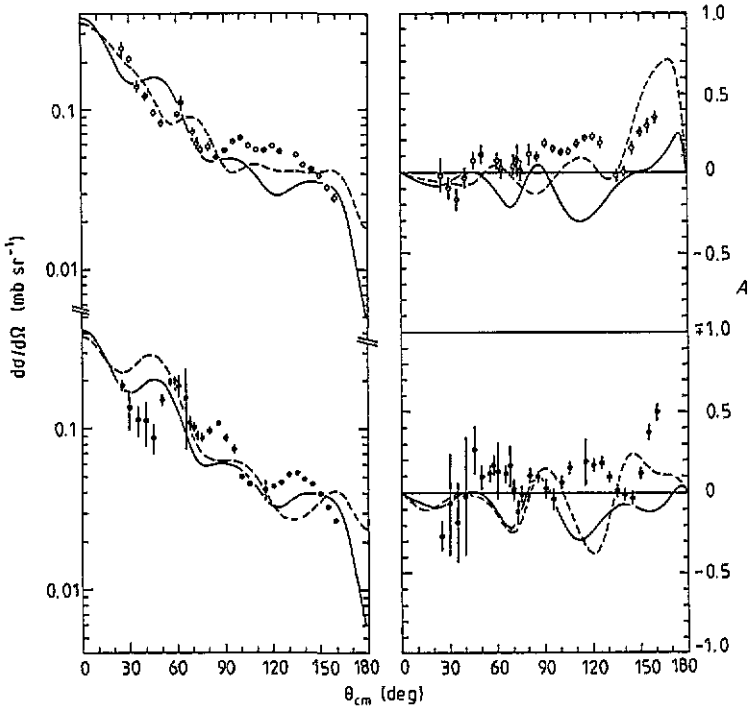

Figure 9. Inelastic scattering from ^{112}Cd (top) and ^{114}Cd (bottom), exciting the 4_1^+ state. Full curves, first-order vibrational model; broken curves, second-order vibrational model. CC scheme: $0230_2 2_2 4$ including one-phonon component mix.

might hope that a destructive interference could reproduce the quite pronounced pattern seen experimentally. We have carried out some calculations using this scheme. The results did not show strong interference effects, the two 0^+ states acting as one effective state. Adding other paths to this coupling scheme did not improve the situation, in particular, it turned out to be impossible to obtain the sharp oscillations in the cross section. This corroborates the nowadays generally accepted interpretation of the 2_3^+ state as the first excited state of the intruder band.

The deformation strength data for this 2_3^+ state are listed in table 5.

In ^{112}Cd we could resolve the 1^- state at 2.507 MeV and the 5^- state at 2.373 MeV (figure 12). We analysed these states as built by a quadrupole and an octupole phonon. In order to obtain the correct magnitude of the cross section we were forced to allow for a direct coupling with the ground state. These direct components actually dominate the cross section and analysing power, which is not surprising from a microscopic point of view because the availability of shell-model orbits with high angular momentum and opposite parity makes direct particle–hole transitions possible that involve a large J transfer. The one-phonon components found in the first-order vibrational calculations have been indicated in figure 12; the deformation data for the 1_1^- and 5_1^- states are listed in table 6.

4. Conclusions

In conclusion, we have measured and analysed a substantial amount of $(\vec{p}, p')$ data on the even cadmium isotopes. The description of the elastic scattering is very satisfactory. Also,

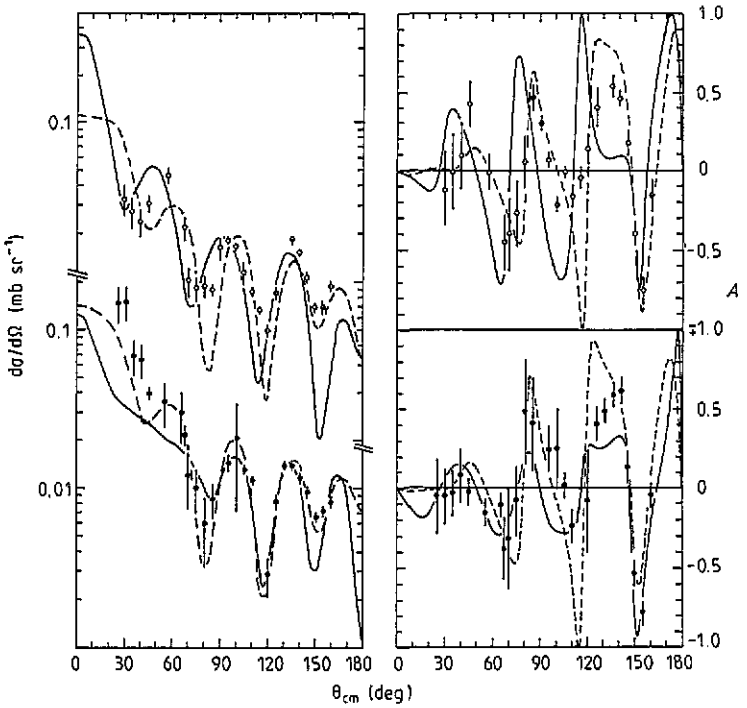

Figure 10. Inelastic scattering from ^{112}Cd (top) and ^{114}Cd (bottom), exciting the 0_2^+ state. Full curves, first-order vibrational model; broken curves, second-order vibrational model. CC scheme: $0230_2 2_2 4$ including one-phonon component mix.

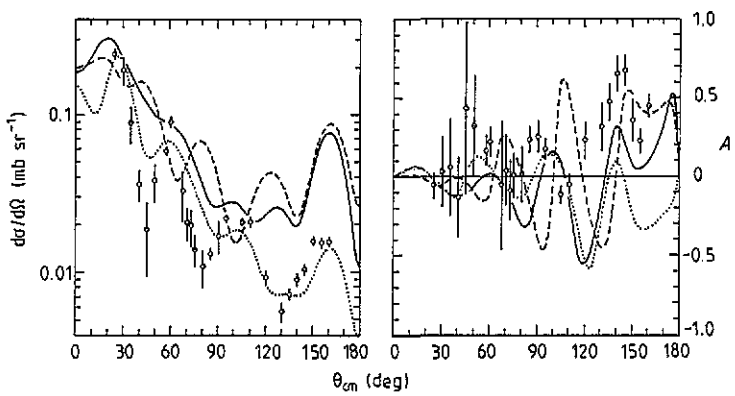

Figure 11. Inelastic scattering from ^{114}Cd, exciting the 2_3^+ state. Full curves, first-order vibrational model; broken curves, second-order vibrational model. CC scheme: 0232_3. The dotted curves result from the simpler scheme 02_3, using the second-order vibrational model (in this simple scheme the first-order model does not deviate significantly from the second-order results except for the analysing power at angles above 145° where the minimum is as low as −0.55).

there is a good agreement between experiment and theory for the 2_1^+ states. The 3_1^- levels, on the other hand, all show analogous discrepancies with theory at backward angles.

The 2_2^+ states exhibit a rather pure vibrational character, which is not completely in line

Table 4. Deformation strengths describing the excitation of the even-mass cadmium isotopes in a two-phonon state of positive parity.

A	Model[a]	β_{0s}	ϕ^{b}_{0s}	β_{2s}	ϕ^{b}_{2s}	β_4	ϕ^{b}_{4}
106	V1			0.16	81	0.025	−37
	V2			0.16	74	0.037	−26
108	V1			0.16	−101	0.054	−81
	V2			0.16	74	0.049	−61
110	V1			0.16	−103	0.129	−85
	V2			0.16	−104	0.125	−99
112	V1	−0.0067	139	0.17	− 99	0.090	−85
	V2	*−0.0060*	*−136*	*0.17*	*−102*	*0.090*	−98
114	V1	0.0073	37	0.18	82	0.070	−80
	V2	0.0077	138	0.18	79	0.059	−27

A	Model[a]	β''_{00s}	β'^{2}_{00s}	$\beta_{02}\times\beta_{20s}$	β''_{02s}	β'^{2}_{02s}	$\beta_{02}\times\beta_{22s}$	β''_{04}	β'^{2}_{04}	$\beta_{02}\times\beta_{24}$
106	V1				0.025		−0.0039	0.020		0.0218
	V2				0.044	0.0070	−0.0059	0.033	−0.011	0.0231
108	V1				−0.031		0.0046	0.008		0.0040
	V2				0.044	0.0071	−0.0060	−0.023	−0.027	0.0124
110	V1				−0.038		0.0054	0.012		0.0025
	V2				−0.040	−0.0066	0.0058	−0.019	0.027	−0.0041
112	V1	*0.0051*		−0.023	−0.026		0.0043	0.008		0.0026
	V2	0.0043	−0.021	−0.021	−0.036	−0.0063	0.0057	−0.012	−0.029	−0.0038
114	V1	0.0058		0.026	0.024		−0.0042	0.012		0.0057
	V2	−0.0057	0.021	−0.019	0.033	0.0058	0.0054	0.052	−0.014	0.0278

No data available for ^{116}Cd.

Notation as in [18] and [19], except that the second and third state of a given angular momentum have been explicitly indicated by the additional subscripts s and t, respectively.

[a] V1, V2 are the first- and second-order vibrational models, respectively.

[b] All ϕ values in degrees.

Table 5. Deformation strength describing the excitation of the third 2^+ ('2t') state in ^{114}Cd.

A	Model[a]	ϕ^{b}_{2t}	β''_{02t}	β'^{2}_{02t}	$\beta_{02}\times\beta_{22t}$	β^{c}_{02t}
114	V1	−86	0.011		−0.00199	0.025
	V2	−90	0.010	0.00018	−0.00018	0.025

See table 4 for notation.

[a] V1, V2 are the first- and second-order vibrational models, respectively.

[b] ϕ-values in degrees.

[c] computed in a 0^+_1–2^+_3 coupling scheme.

β-value for the 2^+_1 state from table 3.

with data from the literature that have been obtained by γ-ray spectroscopy.

The 0^+_2 states in ^{112}Cd and ^{114}Cd, usually considered as 2p4h intruder states, lead us to the conclusion that there is a strong mixing between the (0^+_2) intruder state and the (0^+_3) member of the 'regular' two-phonon triplet.

The 1^-_1 and 5^-_1 states in ^{112}Cd were described by coupling of a quadrupole and an octupole phonon, but could only be reproduced satisfactorily when a direct coupling to the ground state was introduced.

Table 6. Deformation strengths describing the excitation of the 1_1^- and 5_1^- states in ^{112}Cd.

A	Model[a]	β_1	ϕ_1^b	β_5	ϕ_5^b	β''_{01}	β'^2_{01}	$\beta_{02} \times \beta_{21}$	β''_{05}	β'^2_{05}	$\beta_{02} \times \beta_{25}$
112	V1	0.034	−22	0.064	15	0.031		0.025	0.062		0.026
	V2	0.040	19	0.059	−10	0.038	0.0090	0.026	0.058	−0.0049	0.027

See table 4 for notation.
[a] V1, V2 = first-, second-order vibrational model.
[b] ϕ values in degrees.
β-value for the 2_1^+ and 3_1^- states from table 3.

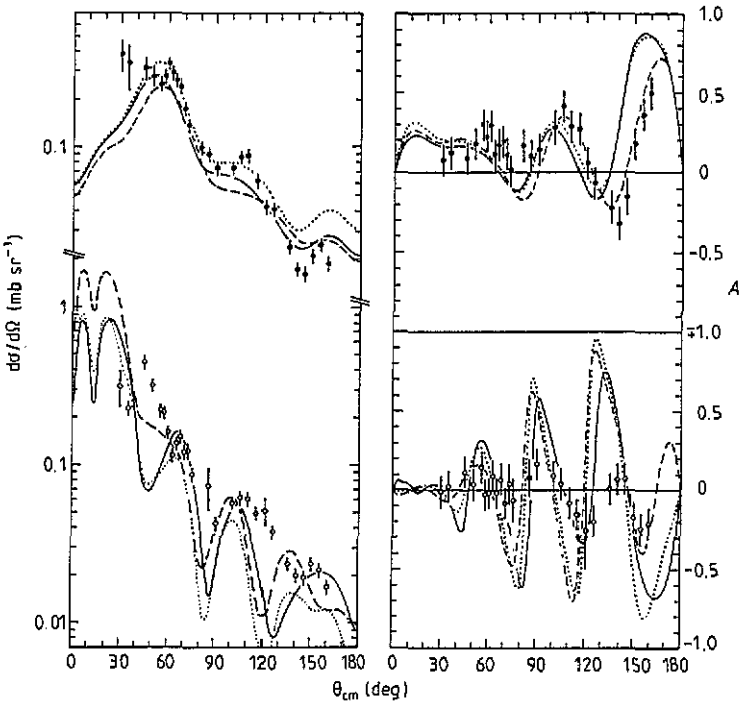

Figure 12. Inelastic scattering from ^{112}Cd, exciting the 5_1^- state (top) and the 1_1^- state (bottom). Full curves, first-order vibrational model; dotted curves, separate one-phonon component of this model; broken curves, second-order vibrational model. cc scheme: 02351.

Acknowledgments

This paper is the last to appear on the work of the former Experimental Nuclear Physics group at this university. We wish to use this opportunity to express our thanks to all members of the technical and administrative staff who have made this work possible during a period of some two decades. Also, we are grateful for the assistance by many students during this time, as well as for the services rendered by the members of the cyclotron maintenance group.

Dr H P Blok's cooperation in some supplementary calculations for this paper is gratefully acknowledged.

This work has been part of the research programme of the Stichting voor Fundamenteel Onderzoek der Materie (FOM), which is financially supported by the Nederlandse Organisatie voor Zuiver Wetenschappelijk Onderzoek (ZWO).

References

[1] Kumpulainen J, Julin R, Kantele J, Passoja A, Trzaska W H, Verho E, Väärämäki J, Cutoiu D and Ivascu M 1992 *Phys. Rev.* C **45** 640

[2] Délèze M, Drissi S, Kern J, Tercier P A, Vorlet J P, Rikovska J, Otsuka T, Judge S and Williams A 1993 *Nucl. Phys.* A **551** 269

[3] Délèze M, Drissi S, Jolie J, Kern J and Vorlet J P 1993 *Nucl. Phys.* A **554** 1

[4] Duval P D and Barrett B R 1982 *Nucl. Phys.* A **376** 213

[5] Heyde K, Van Isacker P, Waroquier M, Wenes G and Sambataro M 1982 *Phys. Rev.* C **25** 3160

[6] O'Donnell J M, Kotwal A and Fortune H T 1988 *Phys. Rev.* C **38** 2047

[7] Casten R F, Jolie J, Börner H G, Brenner D S, Zamfir N V, Chou W-T and Aprahamian A 1992 *Phys. Lett.* **297B** 19 (erratum 1993 **300B** 411)

[8] Wassenaar S D, Van Hall P J, Klein S S, Nijgh G J, Polane J H and Poppema O J 1989 *J. Phys. G: Nucl. Part. Phys.* **15** 181

Van Hall P J, Wassenaar S D, Klein S S, Nijgh G J, Polane J H and Poppema O J 1989 *J. Phys. G: Nucl. Part. Phys.* **15** 199

Wassenaar S D 1982 *PhD Thesis* Eindhoven University of Technology

[9] Petit R M A L, Moonen W H L, Van Hall P J, Klein S S, Nijgh G J, Van Overveld C W A M and Poppema O J 1986 *J. Phys. Soc. Japan* **55** Suppl. p. 594

[10] De Frenne D, Jacobs E, Verboven M and De Smet G 1988 *Nucl. Data Sheets* **53** 73 ($A = 106$)

[11] Haese R L, Bertrand F E, Harmatz B and Martin M J 1982 *Nucl. Data Sheets* **37** 289 ($A = 108$)
Blachot J 1991 *Nucl. Data Sheets* **62** 803 ($A = 108$; update)

[12] De Gelder P, Jacobs E and De Frenne D 1983 *Nucl. Data Sheets* **38** 545 ($A = 110$)
De Frenne D and Jacobs E 1992 *Nucl. Data Sheets* **67** 809 ($A = 110$; update)

[13] De Frenne D, Jacobs E and Verboven M 1989 *Nucl. Data Sheets* **57** 443 ($A = 112$)

[14] Blachot J and Marguier G 1990 *Nucl. Data Sheets* **60** 139 ($A = 114$)

[15] Blachot J, Husson J P, Oms J, Marguier G and Haas F 1981 *Nucl. Data Sheets* **32** 287 ($A = 116$)
Blachot J and Marguier G 1990 *Nucl. Data Sheets* **59** 333 ($A = 116$; update)

[16] Moonen W H L, Van Hall P J, Klein S S, Nijgh G J, Van Overveld C W A M, Petit R M A L and Poppema O J 1993 *J. Phys. G: Nucl. Part. Phys.* **19** 635

[17] Manufactured by Enertec

[18] Tamura T 1966 *Progr. Theor. Phys. Suppl.* **37, 38** 383

[19] Lombard R M and Raynal J 1973 *Phys. Rev. Lett.* **31** 1015

[20] Petit R M A L 1985 *PhD Thesis* Eindhoven University of Technology

[21] Petit R M A L, Van Hall P J, Klein S S, Moonen W H L, Nijgh G J, Van Overveld C W A M and Poppema O J 1993 *J. Phys. G: Nucl. Part. Phys.* **19** 2093

[22] Van Overveld C W A M and Van Hall P J 1984 *J. Phys. G: Nucl. Phys.* **10** 193
Van Overveld C W A M 1985 *PhD Thesis* Eindhoven University of Technology

[23] Van Overveld C W A M 1986 *J. Phys. G: Nucl. Phys.* **12** 167

[24] Lutz H F, Bartolini W and Curtis T H 1969 *Phys. Rev.* **178** 1911

[25] Makofske W, Savin W, Ogata H and Kruse T H 1968 *Phys. Rev.* **174** 1429

[26] Cereda E, Pignanelli M, Micheletti S, Von Geramb H V, Harakeh M N, De Leo R, D'Erasmo G and Pantaleo A 1982 *Phys. Rev.* C **26** 1941

[27] Pignanelli M, Micheletti S, Cereda E, Harakeh M N, Van der Werf S Y and De Leo R 1984 *Phys. Rev.* C **29** 434

[28] De Leo R, Blasi N, Micheletti S, Pignanelli M, Borghols W T A, Schippers J M, Van der Werf S Y, Maino G and Harakeh M N 1989 *Nucl. Phys.* A **504** 109

[29] Wesseling J, De Jager C W, Van der Laan J B, De Vries H and Harakeh M N 1991 *Nucl. Phys.* A **535** 285